EXTRACELLULAR EXPRESSION, OXIDATION AND PURIFICATION OF HEN EGG WHITE LYSOZYME DOUBLE MUTANT (H15S+N77H)

by

Susmita Kapavarapu

Submitted in Partial Fulfillment of the Requirements

For the Degree of

Master of Science

In the

Chemistry

Program

YOUNGSTOWN STATE UNIVERSITY

December, 2007

Extracellular Expression, Oxidation and Purification of Hen Egg White Lysozyme Double Mutant (H15S+N77H)

Susmita Kapavarapu

I hereby release this thesis to the public. I understand this thesis will be made available from Ohio**Link ETD** center and the Maag Library Circulation Desk for public access. I also authorize the University or other individuals to make copies of this thesis as needed for scholarly research.

Signature:

_____

Susmita Kapavarapu Date

Approvals:

_____

Dr. Michael A. Serra Date
Thesis Advisor

_____

Dr. Daryl Mincey Date
Committee Member

_____

Dr. Timothy R. Wagner Date
Committee Member

_____

Dr. Peter J. Kavinsky Date
Dean of Graduate Studies

Thesis abstract

Metal catalyzed oxidation may result in structural damage to proteins and has been implicated in aging and disease, including neurological disorders like Alzheimer's. The selective modification of specific amino acid residues with high metal ion affinity leads to subtle structural changes that are not easy to detect and may have dramatic consequences on physical and functional properties of the oxidized protein molecule. This thesis is about the investigation of the site specificity of metal catalyzed oxidation of the H15S+N77H double mutant of hen egg white lysozyme.

An extracellular mutant was generated using the PCR overlap extension method. The mutant was cloned into the pCR® 4-TOPO® vector. Sequencing showed the successful generation of an H15S+N77H double mutant capable of extracellular expression into pPICZα B vector. The double mutant gene insert was digested out of pCR® 4-TOPO® vector and ligated in the pPICZα B vector.

Future work includes the linearization of pPICZα B and transformation into X-33 competent cells, followed by the extracellular expression of mg quantities of the mutant protein. The results of metal catalyzed oxidation experiments will be compared to those of the native enzyme to reach conclusions about the relationships between site-specific oxidation and protein structure.

Acknowledgements

I would like to express my gratitude to my advisor, Dr. Michael A Serra, for his patience, time and assistance in accomplishing my thesis. I would also like to thank Dr. Mincey, Dr. Wagner for being on my thesis committee and Dr. Caguiat, Dr. Julio Ed. Budde and Dr. Cooper for their help and suggestions.

I would like to offer my special thanks to my mom and dad for their constant support, suggestions and for believing in me. I am much in debt to my dearest brother Sunil Chaitanya for his emotional support, advice and patience (I was quite a handful for him and am still, I guess). I would especially like to extend my sincere gratitude to my friend's Vineela, Seshu, Bhargavi, Ujwala, and Sowmya for all their help.

Finally, I offer my sincere thanks to the School of Graduate studies at YSU for offering me financial assistance without which nothing would have been really possible.

Table of Contents

List of Figures

List of Symbols and Abbreviations

α	Alpha
β	Beta
γ	Gamma
ε	Epsilon
µ	Micro
µg	Microgram
µl	Micro liter
µM	Micro molar
®	Registered
TM	Trademark
%	Percent
Abs	Absorbance
bp	Base pair
BSA	Bovine serum albumin
Cu	Copper
DOPA	Dihydroxy phenyl alanine
DNA	Deoxyribonucleic acid
dNTP	Deoxynucleotide triphosphate
EDTA	Ethylenediaminetetraacetic acid
Fe	Iron
hr	Hour
His	Histidine
Asn	Aspergine
LDL	Low density lipoprotein
Lys	Lysine
kb	Kilo base
LB	Luria-Bertini
M	Molar
MCO	Metal catalyzed oxidation

Met	Methionine
mg	Milligram
min	Minutes
ml	Milliliter
ng	Nanogram
O_2	Oxygen
PCR	Polymerase chain reaction
p^H	Hydrogen ion activity
rpm	Revolutions per minute
s	Second
SOD	Superoxide dismutase
TAE	Tris-acetate buffer
UV	Ultraviolet
V	Volts
v/v	Volume per volume
w/v	Weight per volume

CHAPTER I: Introduction

Partial reduction of molecular oxygen generates a family of reactive compounds known as reactive oxygen species (ROS). ROS have been of interest for many years in all areas of biology. Originally it was thought that ROS were released only by phagocytic cells during the host cell defense mechanism. It is now a well known fact that ROS are released in various biological systems, which includes both animals and plants. ROS include the superoxide radical ($O_2^{\cdot -}$), hydrogen peroxide (H_2O_2), hydroxyl radical ($OH^{\bullet}$) and the lipid peroxides (LOOH). The superoxide radical formed in living organisms has many deleterious effects on biological systems. Evidence proves that systems generating superoxide radical can form the hydroxyl radical. Production of $OH^{\bullet}$ was however, inhibited by the presence of catalase enzyme suggesting that H_2O_2 is required for its production.[1]

These ROS are produced from variety of sources including environmental and physiological pathways like the action of oxidase enzymes. ROS are also present as pollutants in the atmosphere, generated as byproducts of normal metabolism and are formed during exposure to X-ray, gamma, visible and UV irradiation. It was found that when brain mitochondrial respiration is inhibited during brain damage there was increased production of ROS. The most significant source of ROS *in vivo* resulted from the reaction of transition metals ions with the endogenously produced H_2O_2. Reaction of the bound metal ion with H_2O_2 leads to the production of $OH^{\bullet}$ that reacts in the immediate vicinity of its site of production (site-specific metal catalyzed oxidation). ROS react with almost all biological molecules including DNA, RNA, carbohydrates, proteins and lipids thus damaging various cells and tissues causing deleterious effects.

Increased production of ROS results in oxidative stress that contributes to a number of pathological processes leading to a variety of diseases. Metal catalyzed oxidation is the most important mechanism for the oxidation of proteins, because of protein's abundance in biological systems and their high rate constants for reaction. Metal catalyzed oxidation may result in structural damage to proteins and has been implicated in aging and diseases, including neurological disorders like Alzheimer's disease. The selective modification of specific amino acid residues with high metal-ion affinity leads to subtle structural changes that are not easy to detect but may have dramatic consequences on the physical and functional properties of the oxidized protein molecule.

REACTIVE OXYGEN SPECIES (ROS)

Oxygen, which is important for the survival of all aerobic cells, sometimes proves to be dangerous too. Reactive oxygen species such as the super oxide radical ($O_2^{\bullet -}$), the hydroxyl radical ($OH^{\bullet}$), and hydrogen peroxide (H_2O_2) are generated from oxygen. ROS react with all classes of biological molecules causing oxidative damage to DNA, lipids proteins.

A radical is a species that contains one or more unpaired electrons. These free radicals have increased reactivity and among them the hydroxyl radical is the most reactive. The $OH^{\bullet}$ radical being the most reactive of all has the tendency to cause breaks in DNA strands, attacks membrane lipids, proteins, purine and pyrimidine bases. The $OH^{\bullet}$ radical usually is not generated *in vivo*, unless there is an increased concentration of metals ions, especially transition metals like copper and iron, present in the body.[2,3]

Oxygen is bi-radical and readily accepts unpaired electrons and thus gets reduced to varying degrees producing toxic ROS like the superoxide radical. A two electron reduction of oxygen produces the peroxide ion which is not a free radical but protonates

at physiological pH forming hydrogen peroxide which readily reacts with the superoxide radical eventually leading to a series of harmful reactions.

Molecular oxygen is first reduced to superoxide radical, which is formed by the one electron reduction of oxygen. This reaction is catalyzed by NADPH oxidase with electrons supplied by NADPH. Further reduction leads to the formation of hydrogen peroxide. The reaction series of oxygen reduction to various ROS is given in equation (1).[4]

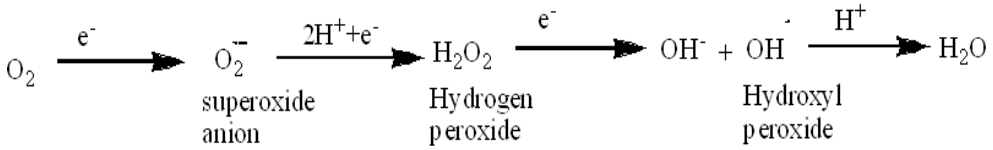

(1)

H_2O_2 formed in the above step is reduced by transition metals like copper and iron to the hydroxyl ion and the hydroxyl radical. Equation (2) shows the reaction with Fe^{2+} and is known as the Fenton reaction which was discovered over a hundred years ago.[5]

$$Fe^{2+} + H_2O_2 \rightarrow Fe^{3+} + OH^- + OH^{\bullet} \qquad (2)$$

Iron in higher oxidation state has to be reduced first to catalyze the reduction of H_2O_2. The Haber-Weiss reaction illustrated in Equation (3) shows how metals in higher oxidation states can be reduced.

$$\begin{aligned} Fe^{3+} + O_2^{\bullet -} &\rightarrow Fe^{2+} + O_2 \\ Fe^{2+} + H_2O_2 &\rightarrow Fe^{3+} + OH^- + OH^{\bullet} \\ \hline O_2^{\bullet -} + H_2O_2 &\rightarrow O_2 + OH^- + OH^{\bullet} \end{aligned} \qquad (3)$$

A similar type of reaction is also observed with copper (I) and hydrogen peroxide. It was also found that the reactivity of copper (I) with hydrogen peroxide is greater than iron (II). The hydroxyl radical diffuses through cell membranes rather easily, so the extent to which the hydroxyl radical can damage the cell depends on how far and how fast it can diffuse through the cell. Hydroxyl radicals have short half -lives and high rate constants. Water can be easily split into the $OH^{\bullet}$ radical by exposure to high-energy radiation. Proteins being the major components of most of the biological systems are the main targets for the ROS. This was also shown by the rate constant data of reaction of various radicals with biological molecules. The rate constant for reaction of $OH^{\bullet}$ with albumin was found to be 8×10^{10} dm^3 mol^{-1} s^{-1}, for DNA it is 8×10^{8} dm^3 mol^{-1} s^{-1}.

The radical reactions are not finished after the initial attack by $OH^{\bullet}$. For example, when an $OH^{\bullet}$ radical attacks a polyunsaturated fatty acid (PUFA) in a membrane lipid, $OH^{\bullet}$ tends to attack the side chains of PUFA and extracts the $H^{\bullet}$ to form water. This reaction removes the $OH^{\bullet}$ but leaves behind another type of radical species, a carbon-centered radical, which undergoes various other reactions forming a peroxy radical. This peroxy radical attacks another membrane fatty acid side chain forming lipid- peroxides thus starting a radical chain reaction known as lipid peroxidation. Lipid peroxidation may inactivate membrane bound enzymes, decreases membrane fluidity, and increases non-specific permeability of ions. In the presence of metal complexes these lipid peroxides decompose to form various other fragments that includes in it more hydrocarbon gases, radicals and aldehydes that are highly toxic even in small amounts.[3,4]

Oxygen is essential for aerobic life but exposure of aerobic living organisms to concentrations above the normal amounts (21%) produces toxic effects. Toxic effects that

are likely to be seen when exposed to abnormal concentrations of oxygen depend also on other factors like species, age, and diet. One of the most medically relevant examples of oxygen toxicity is the retinal damage that can occur in premature babies if the O_2 concentration in the incubator is not controlled properly. This medical condition is known as “retrolental fibroplasias” and arises when the blood oxygen tension is not maintained at optimal concentrations. The damaging effects of elevated oxygen levels are due to the production of superoxide radical ($O_2^{\bullet -}$) in the cells. Oxygen radicals are produced by various systems present in living organisms. For example, electrons that are passing through the mitochondrial electron transport chain directly leak onto O_2 producing the superoxide radical ($O_2^{\bullet -}$) instead of reaching cytochrome *c* oxidase. The concentration of $O_2^{\bullet -}$ radical increases with the increase in concentration of oxygen, hence, if oxygen concentration in the mitochondria is increased, there is an increase in the leakage of electrons from the electron transport chain. $O_2^{\bullet -}$ radical producing systems usually do a great deal of damage to biological systems. Bacterial strains, animal cells in culture, DNA or hyaluronic acid are degraded, damaged or killed when exposed to systems generating superoxide radical.

$OH^{\bullet}$ radicals can be measured using an electron-spin resonance (ESR) spin trapping technique, where the $OH^{\bullet}$ reacts with a spin trap to produce a stable radical with a well defined ESR signal. In another method the $OH^{\bullet}$ radical is allowed to react with an aromatic ring structure such as benzoic acid, phenylalanine or phenol. A set of hydroxylated products are obtained which are then separated using high performance liquid chromatography (HPLC) and quantified using electrochemical detection.

ANTI-OXIDANT DEFENSE MECHANISIM

A number of antioxidant defense mechanisms evolved in living organisms to remove the ROS. Copper is an essential but potentially toxic metal. The concentration of copper increases in the plasma during diseases such as diabetes, oxidative stress, with aging, and during periods of ischemia-reperfusion. These free metal ions will bind to biological molecules and will react with H_2O_2 leading to the production of the hydroxyl radical which reacts in the immediate vicinity of its site of production. Under normal conditions the concentration of free metal ions in blood plasma is usually very low due to the presence of metal binding proteins. For example, metallothionein (MT) binds copper ions preventing the formation of ROS. Sequestering metals acts as an important anti-oxidant defense mechanism.[27]

ROS readily oxidizes methionine to methionine sulfoxide as methionine has a very low oxidation potential. The repair enzyme methionine sulfoxide reductase has the ability to reduce oxidized methionine back to methionine. This plays an important role in protecting the functional residues from oxidative damage and thus acts as an antioxidant.[2]

There are a number of enzymes that play an important role in anti-oxidant defense mechanism. Superoxide dismutase (SOD), a mitochondrial enzyme removes $O_2^{\bullet -}$ by converting it into H_2O_2.

$$O_2^{\bullet -} + O_2^{\bullet -} + 2H^+ \rightarrow H_2O_2 + O_2 \qquad (4)$$

Superoxide dismutase could be considered as a specific catalyst that removes $O_2^{\bullet -}$ by converting it into H_2O_2. The H_2O_2 formed is removed by other enzymes like catalase and glutathione peroxidase (GSHPX) which uses H_2O_2 to oxidize reduced glutathione and

thus removing H_2O_2. Superoxide dismutase is an intracellular enzyme and only small amounts of it are found in plasma fluids, synovial or cerebrospinal fluid. Superoxide dismutase functions as an important biological fluid.

Another technique known to control oxidative damage is the use of chelating agents. Desferrioxamine, one of several inhibitory chelators, is approved for clinical use in iron overload, this is also very specific for iron than any other chelators that are found to be protective. Apart from being a powerful chelator of Fe^{3+}, desferrioxamine acts as a direct scavenger for $OH^{\bullet}$ with a high rate constant and is also a powerful inhibitor of $OH^{\bullet}$ production and Fe dependant lipid peroxidation. Its reaction with $O^{2\bullet -}$, however, has a fairly low rate constant.

METAL CATALYZED OXIDATION (MCO)

Hydroxyl radicals are produced as a result of the reaction between metal ions and H_2O_2 and this process is known as metal catalyzed oxidation. Because of their abundance in biological systems and high rate constants for reaction, proteins are major targets for oxidants. Studies have shown that oxidation of proteins can lead to hydroxylation of aromatic groups, aliphatic amino acid side chain, nitration of aromatic amino acid residues, sulfoxidation of methionine residues, chlorination of primary amino groups and aromatic groups, conversion of some amino acid residues to carbonyl derivatives and formation of cross linked protein aggregates. Oxidation can also lead to the cleavage of the polypeptide chain. Functional groups of proteins may also react with the oxidation products of polyunsaturated fatty acids and carbohydrate derivatives.

Oxidation of side chains of a few amino acids like arginine, lysine, and proline residues yielded carbonyl derivatives. Site-specific damage to proteins is characterized by: 1) modification of one or only a few amino acid residues, 2) oxidative damage that is

insensitive to the presence of free radical scavengers suggesting that radical damage occurs on the surface of the protein but not in the bulk solution and, finally, 3) most of the enzymes that are sensitive to metal ions and H_2O_2 require metal ions for activity. In *E. coli* glutamine synthetase, the amino acids histidine and arginine are closely situated to metal binding sites and are sensitive to site-specific metal catalyzed oxidation which resulted in the loss of activity of these enzymes. Human growth hormone protein (rhGH) contains a well characterized metal binding site, consisting of histidines 18 and 21 which are located on the same side of helix I and glutamic acid 174 on helix IV in the four helix bundle protein. An ascorbate/Cu^{2+} system converted histidine 18 and 21 to 2-oxo-histidine, whereas a surface exposed histidine residue, which was not a apart of the metal binding site, was resistant to MCO. The site-specific nature of MCO has been used as a tool to map the metal binding sites of proteins.[3,6]

When Cu and Zn superoxide dismutase was exposed to hydrogen peroxide, initial cleavage occurred between Pro62-His63 residues which were followed by a random degradation. Compounds like EDTA block random oxidation whereas the catalase enzyme inhibits both random and site specific oxidation.

OXIDATIVE STRESS

Antioxidant defense mechanisms and ROS generation are more or less balanced in biological systems. When this balance is disturbed the concentrations of ROS increases causing oxidative stress. Oxidative stress is involved in several types of neurodegenerative disorders like Parkinson's, Alzheimer's and stroke. The efficiency of certain anti-oxidant defense mechanisms decreases during aging and allows for an increase of ROS production and oxidative stress in aged tissues. Old animals are more

prone to oxidative stress than young ones. Oxidative stress leads to oxidative damage of DNA, proteins, and lipids.

Exposure of cell cultures and animals to different conditions of oxidative stress leads to increased levels of protein carbonyls. The carbonyl content of proteins are increased in human plasma exposed to cigarette smoke, in neutrophils and macrophages, during periods of oxidative burst, in human plasma and rat neurofilaments upon exposure to mixed function oxidation (MFO) systems, and in the liver of mice following exposure to alcohol. Protein carbonyls are also increased in the synovial fluids of patients with rheumatoid arthritis and in the crystalline protein of the human eye lens during cataractogenesis, indicating that the levels of protein carbonyl increased during diseased conditions. It was found that individuals suffering from certain types of diseases like the two premature aging diseases Werner's syndrome and Progeria have levels of protein carbonyls similar to those found in 80-year old persons. Oxidative stress induces apoptosis through an intrinsic pathway where mitochondria play an important role, which is governed by pro and anti-apoptotic proteins that belong to the Bcl-2 family of proteins. Oxidative stress also causes senescence in normal human fibroblasts, when they are exposed to sub-lethal doses of ROS. However, the basic mechanism that is involved in the senescence and apoptosis is still unclear.

Chronic diseases of remote organ systems exert pathological effects on skeletal muscle and these effects were mediated by the systemic transmission of oxidative stress from remote organs through radical inducing substances like cytokines, and metabolic bi-products. Oxidative stress on muscle leads to increased protein degradation, reduced protein synthesis and, thus, to muscle wasting (Figure 1-1).[8,9] Exercise and nutritional

interventions mainly target redox imbalance and protein degradation and pharmaceutical interventions target inflammation and protein degradation.

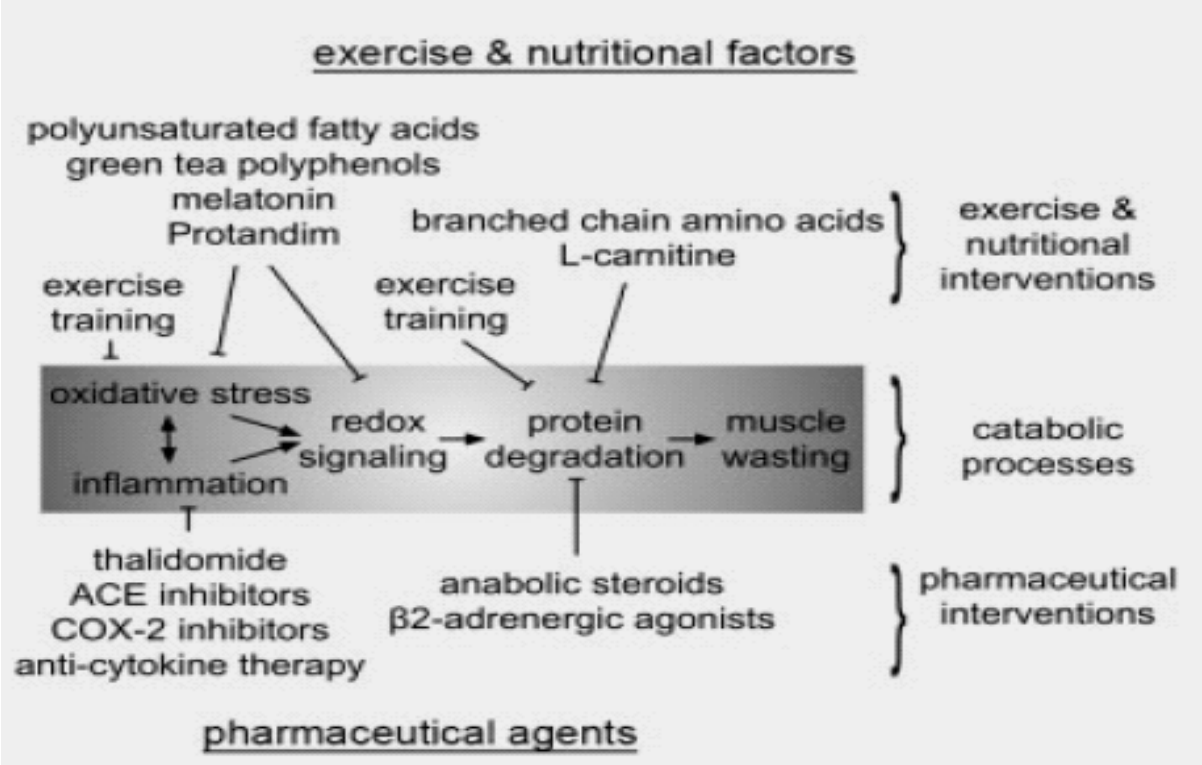

Figure 1-1: Muscle wasting interventions

Dityrosine was released when hydrogen peroxide treated oxy-hemoglobin was incubated with proteases, and its production was inhibited when protease inhibitors were used. Thus dityrosine was not only used as a marker for oxidative damage but is also used as a specific marker for the selective degradation of oxidatively modified proteins. Methionine sulfoxide is yet another potential marker used for oxidative damage and is an oxidation product of methionine.

PROTEIN MODIFICATIONS

ROS may alter every level of protein structure. Oxidation of proteins can have a wide range of downstream consequences. Oxidation may result in the major physical

changes in the structure of the protein ranging from backbone fragmentation to the oxidation of side-chain.

Peptide bond cleavage

Oxidation of proteins by ROS can lead to the cleavage of peptide bonds. The alkoxy radicals alkylperoxide derivatives of proteins undergo cleavage by diamide or α-amidation pathways. In the diamide pathway, the C- terminal amino acid of the fragment derived from the N-terminal portion of the protein will exist as the diamide derivative and the N-terminal portion of the fragment derived from the C-terminal region of the protein will exist as the isocyanate derivative via the diamide pathway (Figure 1-2).[3]

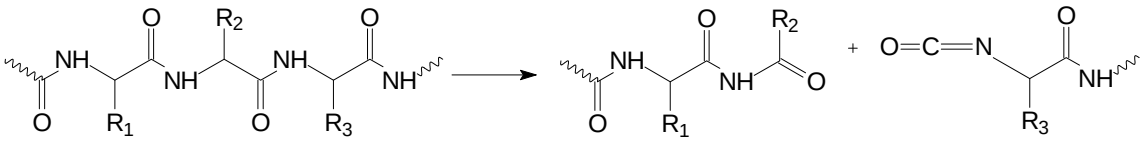

Figure 1-2: Diamide pathway

In the α-amidation pathway, the C-terminal amino acid fragment derived from the N-terminal region of the protein will exist as the amide derivative and the N-terminal part of amino acid derived from the C-terminal fragment will exist as the α-keto-acyl derivative.

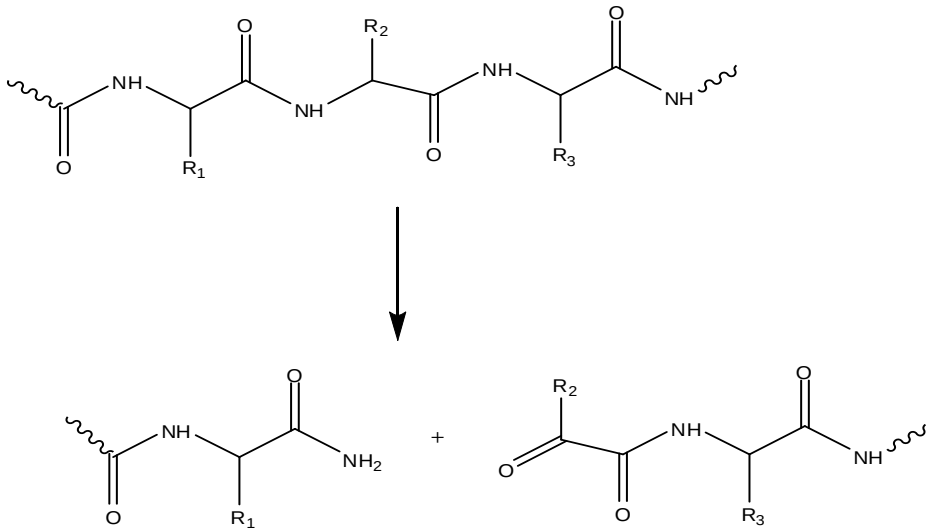

Figure 1-3: α-amidation pathway

Oxidation of aspartyl and glutamyl protein residues also leads to peptide bond cleavage in which the N-terminal amino acid of the C- terminal fragment will exist as N-pyruvyl derivative.

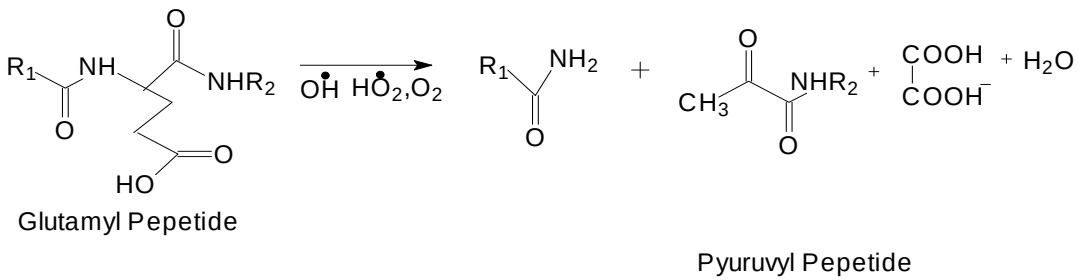

Figure 1-4: Peptide bond cleavage by glutamyl residue.

Schuessler and Schilling proposed that oxidation of prolyly residues may lead to protein fragmentation. This was later verified by showing that the oxidation of proline residues lead to peptide bond cleavage that involved the oxidation of proline residues of

the protein to the 2-pyrrolidone derivative. Acid hydrolysis of the 2-pyrrolidone derivative lead to the formation of 4-amino butyric acid.[3]

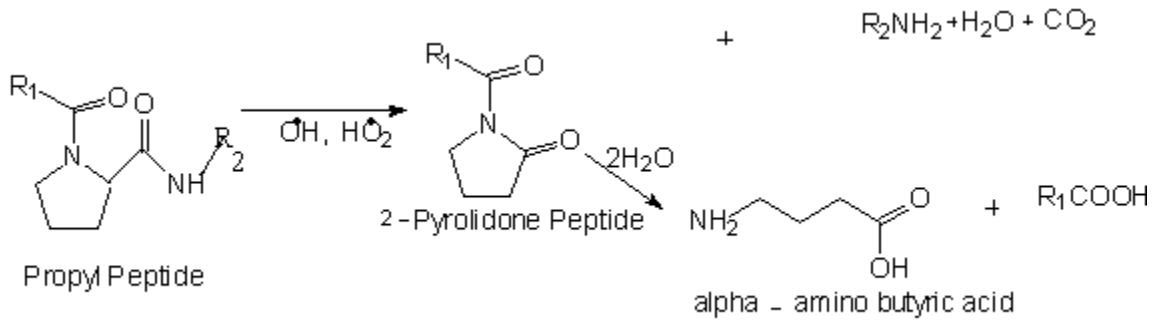

Figure 1-5: Oxidative cleavage of prolyl residues.

Protein-protein cross linkage

Protein-protein cross linked derivatives can be formed by a variety of oxidative mechanisms. One such mechanism involves the interaction of the aldehyde group of 4-hydroxy-2-nonenal (HNE)-protein, a product of lipid per oxidation, with the ε-NH_2 group of a lysine residue in another protein.[1, 5]

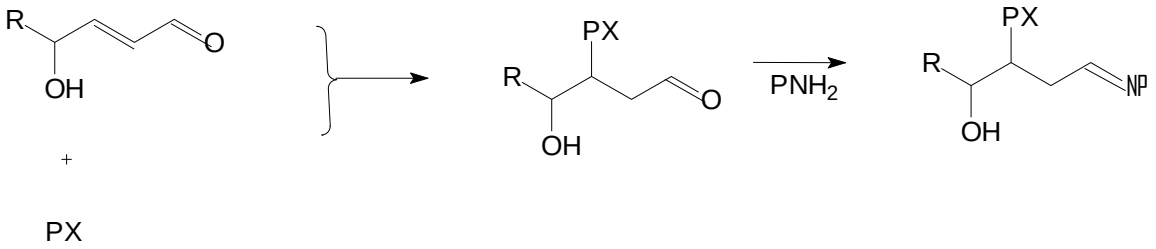

Figure 1-6: Generation of protein-protein cross-linkages by the introduction of carbonyl groups of proteins

Cross-linked proteins often show potential resistance to proteolytic degradation. Thus cross-linked complexes may have important implications in the accumulation of

oxidized proteins that occurs in aging and other diseases. Degradation of oxidized forms of some protein by certain types of proteases may be well inhibited by these cross-linked proteins.

Oxidation of aromatic amino acids

The aromatic amino acid residues are oxidized by various forms of ROS. Tyrosine derivatives are oxidized and converted to a 3,4-dihydroxyphenylalanine (dopa) derivative. Phenylalanine derivatives were oxidized to *ortho*- and *meta*- tyrosine derivatives (Figure 1-7).

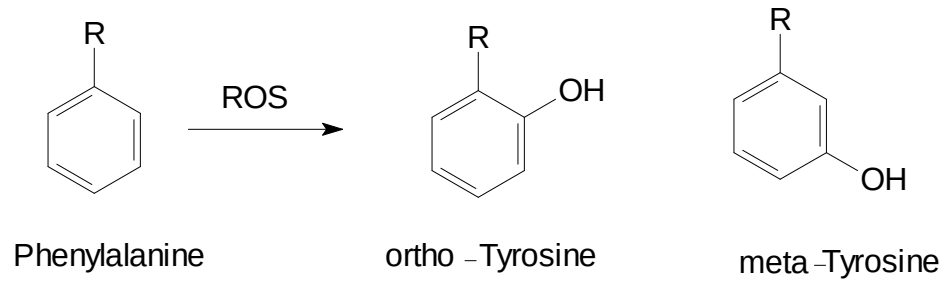

Figure 1-7: Oxidation of phenylalanine

Oxidation of amino acid side chains

MCO oxidation systems can readily oxidize various amino acid side chains. The most susceptible side chains to oxidation include histidine, lysine, cysteine, methionine, proline, and tryptophan. When lysine residues were oxidized with Fe (II) the product formed reacted with hydrogen peroxide generating a hydroxyl radical which then attacks the lysine moiety leading to its conversion to 2-amino-adipic-semmialdehyde.[10]

Formation of further reactive species

When amino acid side-chains and the backbone were oxidized it resulted in the formation of other reactive species. Reactive species that are formed include peroxides, chloramines/chloramides, hydroperoxides, broamines/bromamides and many other short lived intermediate products. The peroxides are formed from the reactions, of tryptophan, tyrosine, and histidine side chains with oxygen. When these reactive species are treated with reducing metal ions or UV light, it was found that they gave further radicals. These secondary radicals were capable of reacting rapidly with molecular oxygen giving rise to superoxide radicals. Formation of further reactive species shows that protein oxidation can occur via chain reactions.

Protein carbonylation

Proteins can be modified by a variety of reactions that involve ROS. Among these reactions carbonylation has a nature that is irreversible and unrepairable. Carbonylated proteins form high molecular weight aggregates that accumulate with age. Such carbonylated aggregates can become cytotoxic and have been associated with a large number of age-related disorders, including cancer, Parkinson's disease and Alzheimer's disease. Carbonyl derivatives are formed by a direct metal catalyzed oxidation attack on the side chains of amino acids like proline, arginine, lysine and threonine. The various possible origins of protein carbonylation includes: (1) increased production of ROS, (2) a decline in the anti-oxidant defense mechanism, (3) increased susceptibility of protein to oxidative attack, (4) decreased capacity for removal of oxidized proteins. All these origins are however only probable possibilities and has evidence both for and against them.[10]

Protein carbonylation is used as an early marker in the oxidation of proteins and is results from oxidative modifications to amino acid residues and by oxidative cleavage of peptide chain.

Unfolding and conformational changes

Unfolding and conformational changes were observed when side chains of proteins are oxidized. These conformational changes have consequential effects on biological systems and their functions. Oxidation of residues that are exposed to the surface have less influence on protein conformation when compared to those residues that are buried. Oxidation processes that take place on side-chains often increase the hydrophilicity of the target residue.

Aliphatic residues are oxidized to peroxides, alcohol, and carbonyl groups whose larger dipole moments participate in hydrogen bonding to solvent molecules and incorporation of polar or charged groups in the case of aromatic residues. Solvent accessible methionine residues are more readily oxidized than that those species that are buried. Met side chains are non-polar in comparison to side-chains of many other amino acids and for this reason these are often found buried within the hydrophobic core of protein structures. Conversion to the more polar sulfoxide has marked effects on conformation. One of the major roles of the Met residue is maintaining a closed hydrophobic pocket that is essential for maintaining the required reduction potential of the protein.[1]

RESEARCH PROBLEM

It has been proposed by some researchers that site specific metal catalyzed oxidation is a caged reaction in which the metal ion binds in a protective pocket on the surface of the protein. This pocket offers a protective shield for the ROS against the antioxidant defense mechanisms. This suggests that the tertiary structure of a protein is important in the process of metal catalyzed oxidation.

Studies have shown that the presence of histidine in the sequence increased protein oxidation significantly. Histidine is one of the most vulnerable amino acids to oxidation reactions. Oxidative damage residues yield 2-oxo histidine as the major product upon incubation with the Cu^{2+}/ H_2O_2/ascorbate MCO system.

A HEN egg white lysozyme double mutant (H15S+N77H) has been developed (Figure 1-8) to investigate what level of protein structure determines the pattern of site-specific oxidation. The native gene contained histidine 15 in a protective pocket but in the mutant gene hisitidine 77 is more accessible to the bulk of the solution.

A different pattern is expected when the histidine 15 is changed to serine and asparagine 77 is changed to histidine. The relationship between the levels of protein structures and sites of oxidation is examined by generating a site directed double mutant of lysozyme to investigate the importance of primary sequence in determining where oxidation occurs

In this thesis, the results of site-directed mutagenesis experiments performed to develop a double mutant gene and expression of mutant lysozyme protein will be discussed.

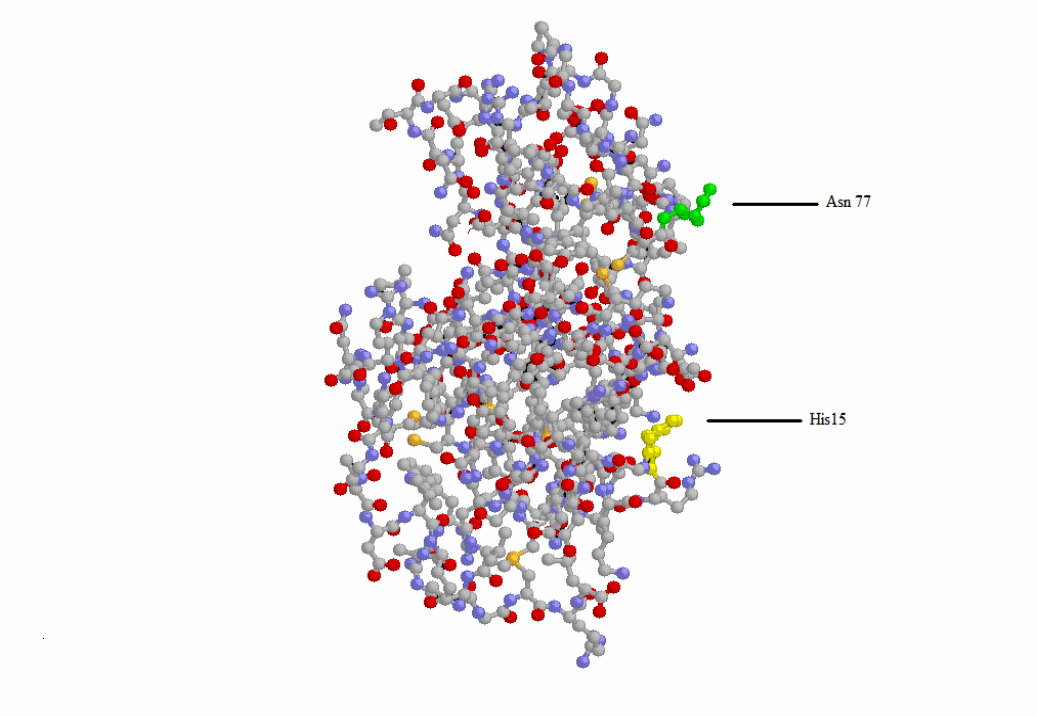

Figure 1-8: Three dimensional structure model of Hen Egg White Lysozyme showing Asn77 (top), and His15 (bottom).

CHAPTER II: MATERIALS AND METHODS

Generation of double mutant

The H15S+N77H double mutant created by a former student, Uma Thatipally, was used as a template for my thesis work. Uma developed a system for intracellular expression. This thesis describes how this system changed to one for extracellular expression. Mutations are generated by changing one or more nucleotides in the gene sequence coding for the amino acid by a method known as base substitution mutagenesis by PCR overlap extension. The goal of this project was to develop a double mutant wherein the histidine codon (CAC) at 15 was converted to a serine codon (AGC) and the asparagine codon (AAC) at 77 was converted to histidine codon (CAC). The gene sequence and corresponding amino acid sequence of native hen egg white lysozyme is given in Appendix A.

The overlap extension method of site-directed mutagenesis includes two PCR steps. The first PCR step utilized the primers N2HR and 5' Ex Lyso for the generation of the front end of the gene, while the second PCR step utilized N2HF and Lyz-R as primers for the generation of the back end of the gene. The synthetic oligonucleotide (Integrated DNA Technologies) primers were designed to introduce the desired point mutations were as follows:

N2HF Forward: 5′ - AAC CTG TGC **CAC** ATC CCG TGC - 3′

N2HR Reverse: 5′ - GCA CGG GAT **GTG** GCA CAG GTT – 3′

The 5' Ex Lyso primer contains a XhoI restriction site for digestion and insertion into pCR® 4-TOPO® vector and then into pPICZα B vector. The sequence of the primer is as follows:

5' Ex Lyso: **5'**- CCCGCC**TCGAG**AAAAGA**AAA**GTCTTTGGACGATGTGAG- **3'**

XhoI starting codon for HEWL

The Lyz-R primer contains an Xba I restriction site and has the following sequence.

Lyz-R 5'- C**TCTA**GAGCCGGCAGCCTC -3

Xba I

The PCR reaction I contained 5 µl of 10 X thermo polymerase buffer (Biolabs), 6 µl of $MgCl_2$, 1 µl of dNTPs (Applied Biosystems), 0.5 µl of Vent polymerase (Biolabs), 0.5 µl N2HR primer (100 µM), 0.5 µl 5' Ex Lyso primer (100 µM), 0.5 µl of pCR® 4-TOPO® plasmid (Invitrogen) with H15S mutant as template and 35 µl of sterile water to give a total volume of 50 µl. The PCR reaction II contained 5 µl of 10 X thermo polymerase buffer, 6 µl of $MgCl_2$, 1 µl of dNTPs, 0.5 µl of Vent polymerase, 0.5 µl N2HF primer (100 µM), 0.5 µl Lyz-R primer (100 µM), 0.5 µl pCR® 4-TOPO® plasmid (Invitrogen) with H15S mutant as template and 35 µl of sterile water to give a total volume of 50 µl.

The thermal cycle (Peltier thermal cycler) program included a 30 sec melting step at 95°C and 35 cycles of the following steps: 95°C for 1 min, 55°C for 1 min, and 72°C for 1 min. A final elongation step at 72°C for 10 min was performed. The front end and back end PCR products were then verified by running a 1% agarose gel at 85V for 1hr in 1x TAE buffer (Tris-acetate buffer). The gel was stained for 15-20 min in a 1x TAE

buffer containing 2µg/mL ethidium bromide solution. The PCR resulted in two fragments. The front end, PCR I was about 250bp while the back end PCR II was approximately 150bp in length. The PCR products were eluted from the gel using Amresco's cyclo-pure Gel Extraction Kit.

The eluted fragments were then annealed by an overlap extension technique and the complete gene was reconstructed. The overlap extension reaction PCR mix contained 5 µl of 10X thermo polymerase buffer, 6 µl of $MgCl_2$, 1 µl of dNTPs, 0.25 µl Taq polymerase (Applied Biosystems), 0.5 µl 5' Ex Lyso, 0.5 µl Lyz-R, 1 µl of front end fragment, 1 µl of back end fragment and 34.75 µl of sterile water to attain a total volume of 50 µl. The thermal cycle program included a 9 min melting step at 95°C and 35 cycles of the following steps: an initial step at 95°C for 1 min, 55°C for 1 min, 72°C for 1 min. and elongation step at 72°C step for 10 min. The reconstructed gene was verified by running a 1% agarose gel before proceeding to the next step.

Preparation of Competent TOP10 *E. coli* cells:

TOP10 *E. coli* cells were streaked out on Luria-Bertini (LB medium) medium plates and grown overnight in the incubator at 37°C. Two colonies were taken and added to 3 ml of LB broth and were grown overnight at 37°C with shaking at 250 rpm. Three milliliters of the overnight culture was taken, added to 100 ml of LB broth and grown at 37°C until the A_{600} was about 1.0. It took about one and a half to two hours to attain an absorbance of 1.0. Cells were then pelleted out at 5000 x g for 5 min. at 4°C. The pellet was resuspended in 10 ml of ice cold 0.15M NaCl, and the cells were re-pelleted. The cells were resuspended in 1ml of ice cold transformation buffer (0.1M $CaCl_2$, 0.01M Tris-HCl, p^H 8.0, 0.01M $MgCl_2$, 15% (v/v) glycerol). Resuspended cells were then

incubated on ice for 30 min. to 2hrs, after which they were stored at -80°C overnight before they were used.

Transformation of One Shot® TOP10 *E. coli* cells:

The annealed mutant lysozyme gene was cloned into the pCR® 4-TOPO® vector (Figure 2-1). The TOPO® vector cloning reaction contained 3 µl of fresh PCR product, 1 µl salt solution (1.3M NaCl, 0.06 M $MgCl_2$), 1µl sterile water and 1 µl of TOPO® Vector. This reaction was incubated on ice for 5-30 min. and used to transform competent cells.

A chemical transformation was performed where 2 µl of the cloning reaction was added to the thawed One Shot® chemically competent TOP10® *E. coli* cells and mixed gently by swirling. The cells were then incubated on ice for 30 min and were heat shocked at 42°C for 30 sec without shaking. The cells were then immediately placed on ice and 250µl of room temperature SOC medium (2% tryptone, 0.5% yeast extract, 10mM NaCl, 2.5mM KCl, 10mM $MgCl_2$, 10mM $MgSO_4$ and 20mM glucose) were added. The reaction mix was incubated at 37°C with shaking at 250 rpm for 1 hr. 50 µl of the above reaction mix was plated on pre-warmed LB plates containing 50 µg/ml ampicillin and incubated at 37°C overnight.

Five double mutant *E. coli* colonies were selected from the LB plates that were kept for overnight growth and labeled as DM1, DM2, DM3, DM4, and DM5. These colonies were grown in 3ml of LB medium containing 50µg/ml ampicillin and grown overnight growth in the incubator at 37°C with shaking at 250 rpm.

Plasmid with our desired mutant gene was then later isolated from the LB medium cultures using Amresco Cyclo-Prep Kit. Double digestion was performed using Xho I and Xba I to verify the presence of the insert in the plasmids before the samples

were sequenced. The double digest mix contained 6 µl DNA sample, 1 µl Xba I, 1 µl Xho I, 2 µl 10x NE buffer (#2), 1 µl BSA (10mg/ml is diluted to 1:10 concentration) and 9 µl of sterile water was added to get a final volume of 20 µl. This reaction mix was incubated for 2 hrs at 37°C. A 1% agarose gel was run at 85 V for 1 hr with the digested sample.

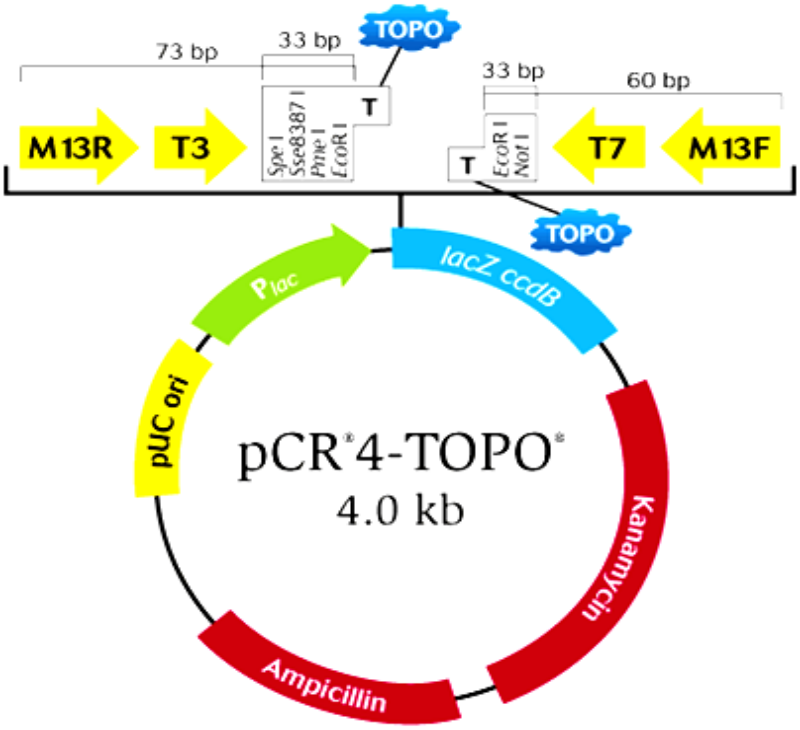

Figure 2-1: The pCR® 4-TOPO® Vector (~4.0Kb) with TOPO® cloning site.

DNA Sequencing

Sequencing was performed on the cloned pCR® 4-TOPO® using the Beckman-Coulter CEQ 2000 Dye Terminator Cycle Sequencing Kit. The sequencing mix consisted of template (mutant and native pCR® 4-TOPO® plasmids) for the synthesis of a complimentary strand, oligonucleotide primers, ddNTPs and dNTPs to use as substrates

for the synthesis. M13 forward and reverse primers that were used in the sequencing reaction are as follows:

M13 Forward: 5'- GTAAAACGACGGCCAG-3'

M13 Reverse: 5'- CAGGAAACAGCTATGAC-3'

Using these primers two sets of reaction mixes were prepared. The first set used M13 forward primer, and the second set used M13 reverse primer. Each reaction contained 7 µl template (160ng), 1µl of the appropriate primer (1.6 µM) and 11 µl of the premix (the DNA sequencing premix included 200 µl 10x sequencing reaction buffer, 100 µl of dNTP mix, 200 µl ddUTP dye terminator, 100 µl ddGTP dye terminator, 200 µl ddCTP dye terminator, 200 µl ddATP dye terminator).

The PCR cycle program included 96 °C for 20 sec, 50°C for 20 sec, and 60°C for 4 min; this was repeated for 30 cycles followed by a hold at 4°C. Ethanol precipitation was then carried out on these samples followed by rinsing and vacuum drying for 30 min or until dry. The pellets were then resuspended in sample loading buffer. The sample preparation was carried out as mentioned and was sent for sequencing.

Ligation of double mutant gene into pPICZα B

After the verification of the sequence of the mutant gene it was ligated into the pPICZα B vector (Figure 2-2). The mutant gene was amplified by PCR. The PCR reaction mix included 25 µl of master mix (Promega), M13 reverse and M13 forward primers (Integrated DNA Technologies), 5 µl of DNA (double mutant gene in pCR® 4-TOPO®), and 18µl of sterile water to bring the volume of the reaction mix to 50µl. The PCR program included the following steps: 95°C for 1 min, 55°C for 1 min, 72°C for 1 min for 35 cycles, after 35 cycles an elongation step at 72°C for 10 min.

The pPICZα B vector

pPICZα A, B, C vectors contain the following functionally tested factors: 5'*AOX*: A 942 bp fragment containing the *AOX1* promoter that allows methanol-inducible, high level expression in *Pichia,* multiple cloning sites with 10 unique restriction sites that allows insertion of the gene of interest into the vector, a native *Saccharomyces cerevisiae* α- factor secretion signal that allows for efficient secretion of proteins from *Pichia,* a C- terminal *myc* epitope tag that permits the detection of fusion protein by the anti-*myc* antibody, a C-terminal polyhistidine tag that permits the purification of recombinant fusion protein on metal- chelating resin such as Probond^{TM} , *AOX1* Transcription termination factor (TT), a transcription elongation factor 1 (P_{TEF1}) gene promoter from *Saccharomyces cerevisiae* that derives the expression of the *sh ble* (*Streptoalloteichus hindustanus ble* gene) gene in *Pichia,* conferring Zeocin^{TM}, a synthetic constitutive prokaryotic promoter that derives the expression of the *sh ble* gene in *E. coli,* a Zeocin^{TM} resistance *sh ble* gene for selection in *E. coli* , 3' end of the *Saccharomyces cerevisiae* CYC1 (cyc1TT) gene that allows efficient 3' m RNA processing of the *sh ble* gene for increased stability, a pUC origin that allows replication and maintenance of the plasmid in *E. coli* and unique restriction sites such as *Sac I, Pme I, BstX I,* that permits linearization of the vectors at the *AOX1* locus for efficient integration into the *Pichia* gene.

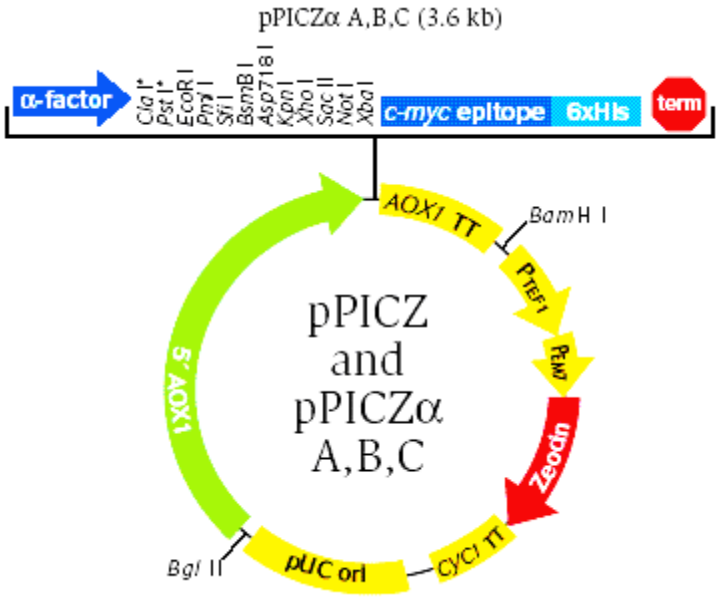

Figure 2-2: The pPICZα A, B, C Vector (3.6kb) used for cloning experiments.

Transformation of JM110 cells with pPICZα B vector

The pPICZα B vector (2µg) from Invitrogen was supplied as a lyophilized powder. The vector was dissolved in 20µl of sterile water to make the final concentration 0.1µg/µl. 50 µl of JM110 competent cells (Stratagene) were placed in three pre-chilled tubes. 0.85µl of β-mercaptoethanol was added to the tubes and incubated on ice with regular swirling of the tubes every 2 min. for a period of 10 minutes. 2µl of the diluted pPICZα B vector was added to the three tubes and further incubated on ice for 30 minutes, and the cells were heat shocked in a 42°C water bath for 45 seconds. The cells were again incubated on ice for 2 minutes, and then 450 µl of SOC media was added. The tubes were incubated in a 37°C shaking incubator for 1 hour. About 100 µl of the mixture from the tubes was taken and plated on low salt LB plates containing 25µg/ml Zeocin™. Colonies from the plates was grown overnight in a shaking waterbath at 37°C

in LB media with 25 µg/ml Zeocin^{TM}. Plasmid from the cells was isolated using a Cyclo-Prep Kit from Amresco. The isolated plasmid was then run on a 1% agarose gel at 85 V for 1 hr and the concentration was estimated by comparing the intensity of the band produced by the isolated plasmid sample to the intensity of a known quantity of DNA.

Restriction digestion was performed on the amplified mutant gene and the isolated pPICZα B vector using the restriction enzymes Xho I and Xba I. The reaction mix contained 3 µl of pPICZα B plasmid (10ng/µl), 7µl of mutant gene (13ng/µl), 2 µl of 10X NE buffer (#2), 0.5 µl of Xho I, 0.5 µl of Xba I, 1 µl of BSA (1:10 diluted) and 6µl sterile water to bring the volume of the reaction mix to 20 µl. The reaction mix was incubated at 37°C for 2 hrs. The digested product was verified by running a 1 % agarose gel.

Ligation was then carried out. The ligation reaction mix contained 3 µl of 10X DNA ligase buffer with 10mM ATP, 10 µl of DNA with insert, 1 µl of T4 DNA ligase, 6 µl of sterile water to bring the volume to 20 µl. The reaction mix was then incubated at 16°C for 12-16 hrs. The reaction was stopped by adding 0.5 µl of EDTA. The ligation mix was stored at -20°C till the commencement of the next step.

Transformation of *E. coli* with the ligated pPICZα B was performed by diluting 2 µl of the ligation mix with 2 µl of sterile water. 2 µl of the diluted mix was then added to 50 µl of JM110 competent cells. The cells were mixed gently by swirling and were incubated on ice or 30 min. The cells were then heat shocked for 30 sec at 42°C. To the heat shocked cells, 250 µl of room temperature SOC medium was added and incubated at 37°C for 1 hr with shaking at 250 rpm. 50 µl of each transformation was spread on pre-

warmed low-salt LB medium plates containing 25µg/ml of Zeocin™ and incubated overnight at 37°C.

Selected colonies from the LB plates were then grown in 5 ml of low-salt LB medium containing 25mg/ml Zeocin™ and grown in a horizontal shaker at 37°C overnight with shaking at 250 rpm. Plasmid was then isolated from the overnight culture using a Cyclo-Prep Kit from Amresco.

PCR was then performed to verify if the *E. coli* was transformed with the pPICZα B containing the desired gene. The PCR mix contained 5 µl of 10 X PCR buffer, 6 µl $MgCl_2$, 1 µl of dNTPs, 0.25 µl of Taq polymerase (Applied Biosystems), 0.5 µl of each Lyz-F and 5'Ex Lyso primer and sterile water to give a total volume of 50 µl. The thermal cycler was programmed at 95 °C for 9min 30s, followed by 35 cycles of 95°C for 30sec, 58°C for 30 sec, 72 °C for 1 min, and a step of 72 °C for 7 min, after the 35 cycles. The PCR products were analyzed using 1% agarose gel.

CHAPTER III: RESULTS

Generation of double mutant

The front end and the back end of the double mutant gene generated by PCR were analyzed by gel electrophoresis. 10 µl of sample obtained by the two PCR reactions were analyzed by running on 1 % agarose gel in 1X TAE buffer. The gel was run at 85 V for 1 hr, and then was soaked in ethidium bromide for 15-20 min. The gel was analyzed using Stratagene imaging system. The gel picture showed the front end of ~ 300bp (Figure 3-1) and the back end of ~ 150bp (Figure 3-2). The band size was compared with a DNA base pair ladder which was also run along with the sample in estimating the size of the bands. Here the 100bp ladder from Amresco was used.

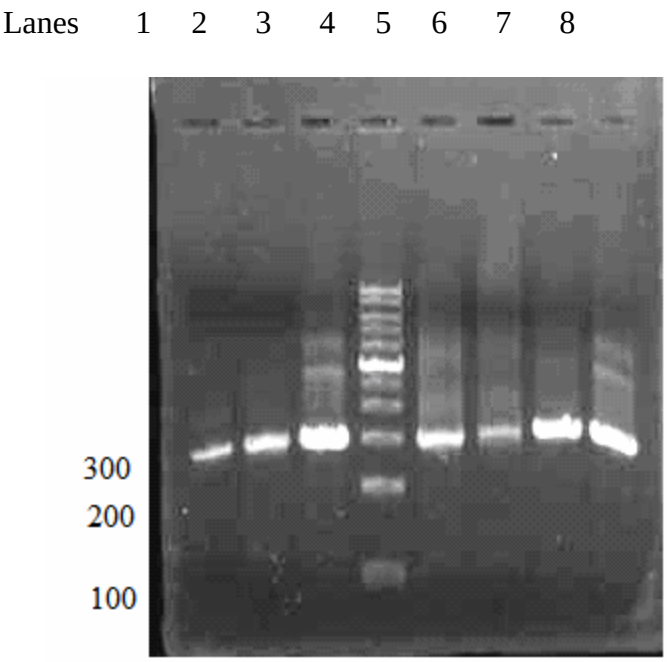

Figure 3-1: 1% agarose gel showing the front end fragments of mutant gene. Lanes 4 show 100 bp ladder, Lanes #1- 3and 5-8 show PCR 1 product (~ 300 bp).

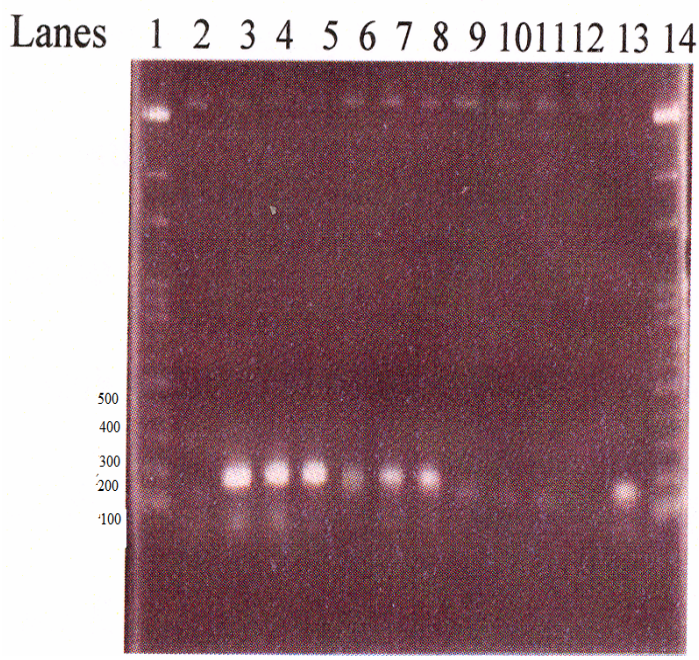

Figure 3-2: 1% agarose gel showing back end fragments of the mutant gene. Lanes 1 and 14 shows the 100 bp ladder, Lanes 3-13 show the back end of the mutant gene (~ 150 bp)

The front and back end fragments were annealed together and the complete gene was constructed. The PCR product was run on 2 % agarose gel at 85V for 60-65 min and stained with ethidium bromide. Figure 3-3 shows the PCR product from overlap extension. The PCR product yielded a gene of about 400 bp showing that the front and back end were annealed successfully.

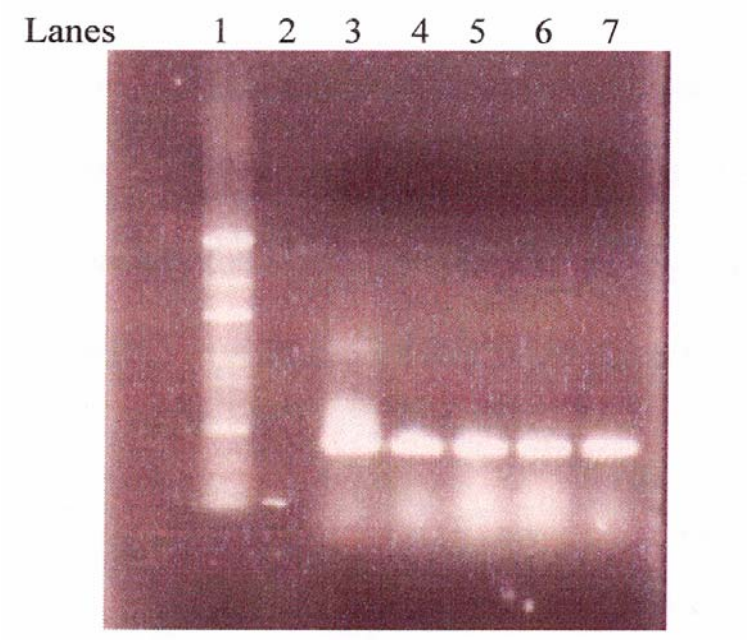

Figure 3-3: Agarose gel picture showing the annealed PCR product. Lane 1 shows the 100 bp ladder and lanes 3-7 shows the annealed mutant gene (~400 bp).

Transformation of TOP10 *E. coli* cells

The mutant gene obtained was cloned into the pCR® 4-TOPO® vector. A linearized pCR® 4-TOPO® vector provided with 3'-T overhangs was supplied in the kit which allows the PCR insert to ligate efficiently with the vector as Taq polymerase used adds the overhanging 3'-adenine residues to the PCR product. After the transformation of TOP10 *E. coli* cells with pCR® 4-TOPO® containing the mutant gene, the transformations were plated on the LB plates. These LB plates were incubated overnight at 37°C. Plates showed growth of ampicillin-resistant *E. coli* colonies. The plasmid with the desired double mutant gene was isolated and the products were run on a 1% agarose gel at 85V to verify the successful insertion of the double mutant gene into the plasmid.

The gel was stained with ethidium bromide and the gel picture that was taken subsequently showed the recombinant plasmid of the expected size (~4400 bp).

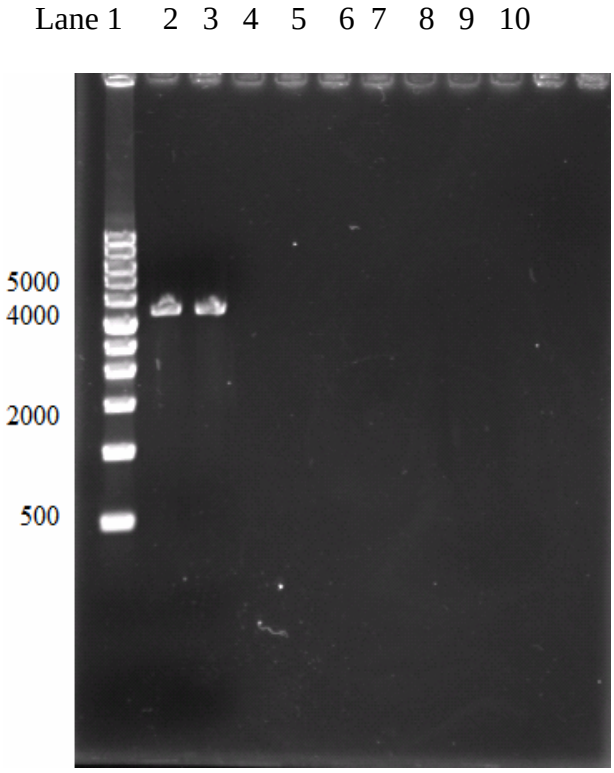

Figure 3-4: 1% agarose gel with plasmid containing the mutant gene. Lane 1 showing 1 kb ladder, lanes 2-3 showing the plasmid with mutant double mutant gene (~4400 bp)

Sequencing results

The hen egg white lysozyme gene contains a total of 387 nucleotides. In the native sequence the codon CAC for residue 15 encodes for histidine and the codon AAC for residue 77 encodes for asparagine whereas in the mutant whereas in the mutant sequence the codon CAC (histidine) is replaced by AGC (serine) and the codon AAC (asparagine) is replaced by CAC (histidine).

Sequencing reactions were performed both on native and mutant genes and the results confirmed the success of the mutagenesis experiments. A portion of the electropherogram is shown below confirming the mutation of the CAC codon for

histidine to AGC for serine and the AAC codon for asparagine to CAC for histidine (Figure 3-5).

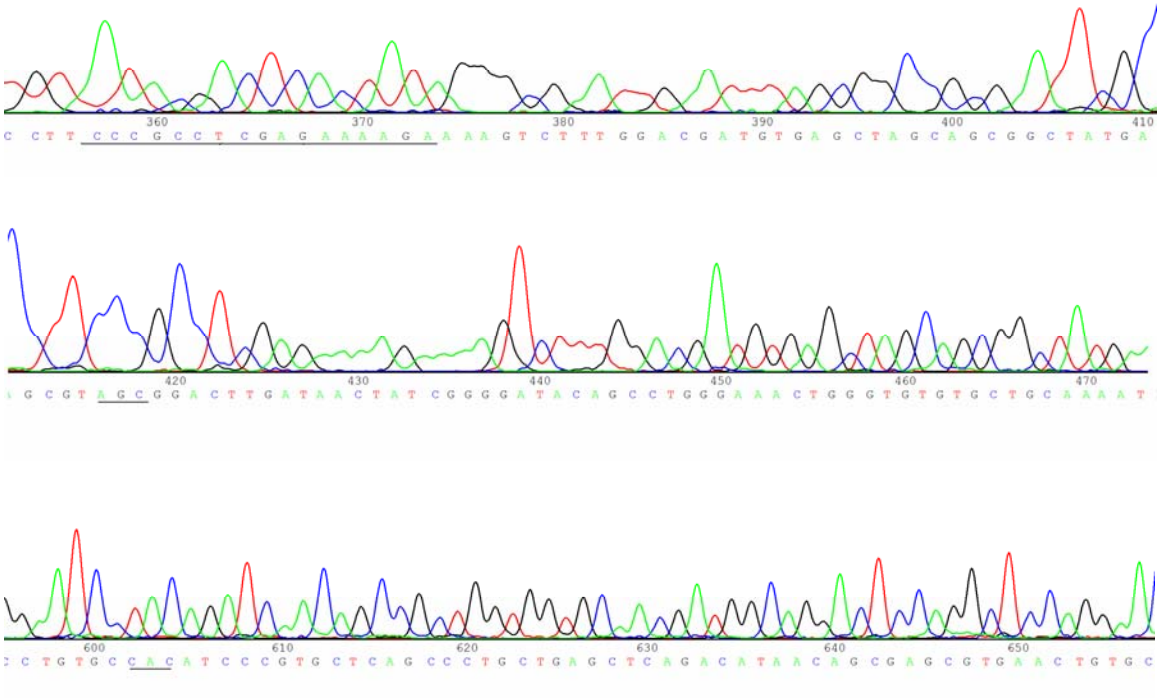

Figure 3-5: Sequence showing 5' Ex Lyso with XhoI (top), sequence showing H15S Mutation (middle), sequence showing N77H mutation (bottom).

Ligation of double mutant gene into pPICZαB and transformation of *E. coli*.

Once the sequence of the mutant gene was confirmed, a double restriction digestion was performed on the isolated plasmid containing the desired gene with Xho I and Xba I. A 400 bp DNA fragment containing the mutant hen egg white lysozyme coding sequence flanked by XhoI and XbaI sites was isolated from the 4000 bp pCR® 4-TOPO®(Figure 3-6).

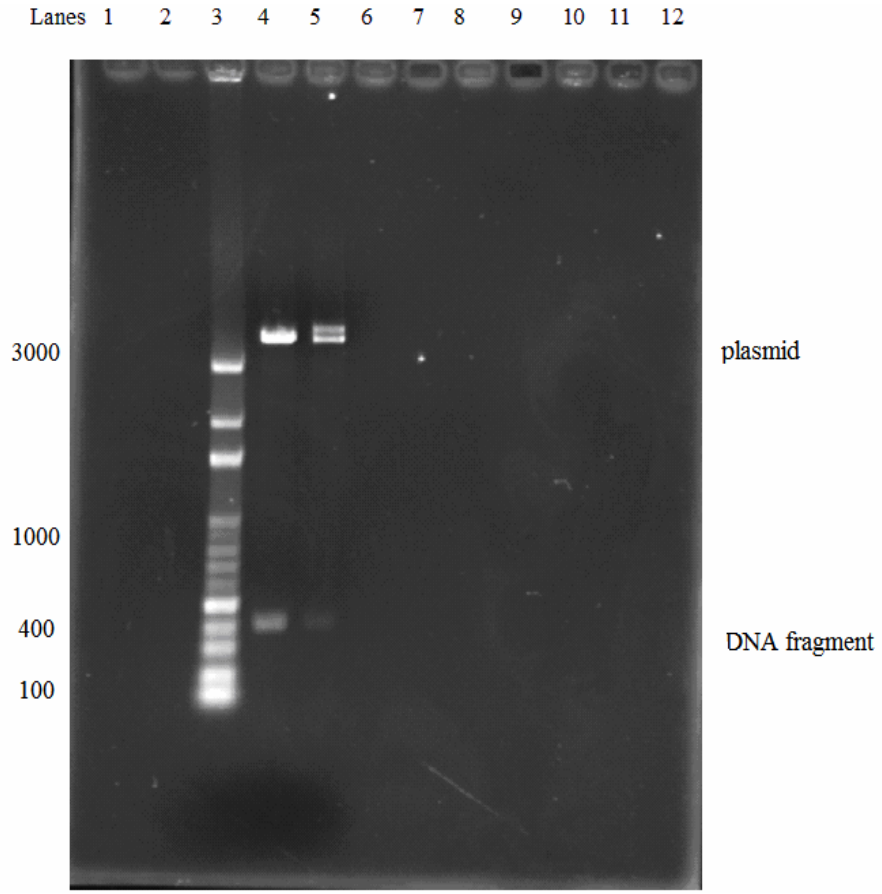

Figure 3-6: Agarose gel showing the 400bp DNA fragment (bottom) and the 4000bp plasmid (top)- Lanes 4 and 5, Lane 3 showing 100 bp ladder

The isolated DNA fragment containing the mutant gene was inserted into the pPICZα B plasmid. First the plasmid containing the mutant lysozyme gene was amplified by PCR and the product was run on 1% agarose gel at 85V to verify the amplification (Figure 3-7).

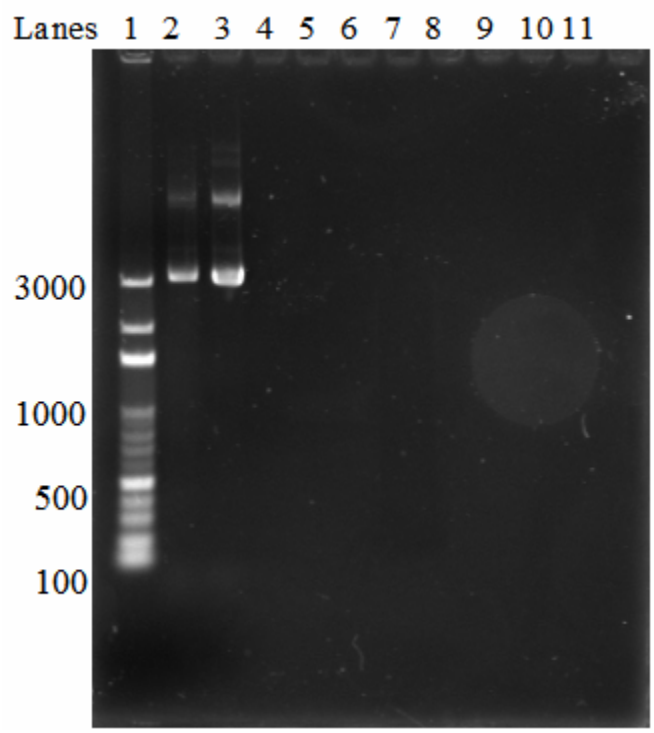

Figure 3-7: Agarose gel picture showing the amplified mutant lysozyme gene in the plasmid (~4400 bp) –Lanes 2 and 3, Lane 1 showing 100 bp ladder

The amplified mutant lysozyme gene was ligated into pPICZα B vector and transformed into TOP10 *E. coli* cells. Cells were incubated at 37°C overnight, plasmid was then isolated from the cells. Finally restriction double digestion was performed using XhoI and XbaI restriction enzymes to verify the presence of the mutant hen egg white lysozyme gene in the pPICZαB vector. The product of the double digest was run on 1% agarose gel at 85 V for 60-65 min showed two bands; one at 4000 bp (pPICZαB vector) and the second one at 400 bp (mutant gene) Figure 3-8.

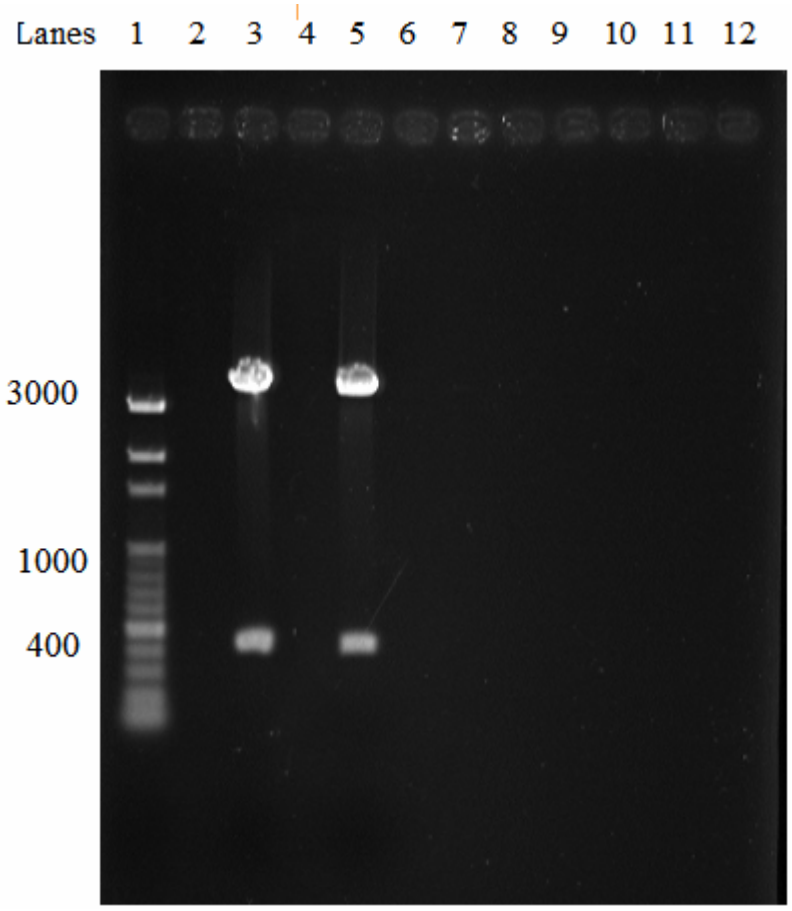

Figure 3-8: Agarose gel showing restriction double digest product. Lane 1 show 100 bp ladder, Lane 3and 5 showing the pPICZαB vector (top) and mutant DNA). gene (bottom).

CHAPTER IV: DISCUSSION

Metal ions bind to biological molecules and react with H_2O_2 producing the $OH^{\bullet}$ which reacts in the immediate vicinity of its site of production. The damage has been referred to as site-specific oxidation. Site-specific metal catalyzed oxidation is perceived as a "caged" reaction where in metal ions bind in a protective pocket found along the protein surface. In the case of some enzymes this type of caged reaction resulted in conversion of some amino acids to carbonyl derivatives, loss of catalytic activity, and an increased susceptibility of protein degradation. To examine what level of structure is important in determining the sites of oxidation caused by the reaction between metal ions and H_2O_2, a double mutant of hen egg white lysozyme was generated.

Hen egg white lysozyme (HEWL) was taken as a model protein for these studies because it is structurally well characterized its primary (Figure 4-1) and tertiary structures are well known and is relatively small protein (129 amino acid residues). HEWL is an extensively studied protein that has been used in various fields of protein research.

To examine what level of protein structure is important in determining the site or sites of oxidation caused by the reaction between the metal ions and H_2O_2. We generated a series of site-directed mutants of HEWL to examine the importance of primary versus tertiary structure. In native lysozyme His 15 is in a protective pocket whereas in our mutant lysozyme His 77 is exposed to the solution. By comparing the oxidation patterns between the native lysozyme enzyme and the double mutant we may predict the role that protein structure plays in site-specific metal catalyzed oxidation.

In this research an H15S+N77H mutant gene capable of extracellular expression was generated by PCR and cloned into a pCR® 4-TOPO® vector. 5' Ex Lyso and Lyz-R were used as primers to produce the front and the back end of the mutant gene. TOP10 *E. coli* was used for transforming the cloned pCR® 4-TOPO® vector and the maintenance of the plasmid. The cloned gene was detected by restriction double digestion with Xho I and Xba I. Further more, the double mutant was confirmed by DNA sequencing.

The ligation of the mutant lysozyme into the XhoI and XbaI restriction site of the pPICZα B vector isolated from *E. coli* cells was not initially successful. Methylation of the Xba I restriction site by methylase activity in TOP10 *E. coli* prevented the cleavage of this site. To overcome this problem the pPICZα B vector was replicated into JM110 competent cells and used for ligating the double mutant into the vector. JM110 competent cells do not have *dam* methylase or *dcm* methylase enzymes thus preventing the Methylation of the Xba I restriction site. Restriction digest with Xho I and Xba I enzymes was now made possible. JM110 cells have a high frequency of recombination, hence TOP10 *E. coli* cells were transformed with the recombinant plasmid.

Future work includes the transformation of the yeast *Pichia pastoris*, followed by small scale expression to determine the optimal growth conditions. Once the growth conditions are optimized, large scale extracellular expression of the protein will be carried out. The expressed protein will be then subjected to metal catalyzed oxidation using the Cu^{+2}/H_2O_2 and the oxidation pattern of the mutant lysozyme will be compared with the native.

Conclusions:

The H15S+N77H HEWL double mutant was successfully generated for extracellular expression. The mutant was subcloned into pCR® 4-TOPO® and subsequently was ligated into pPICZα B vector. Future work has to be carried out on protein expression, metal catalyzed oxidation experiments and then finally comparing the oxidation patterns of the double mutant H15S+N77H with the native HEWL lysozyme.

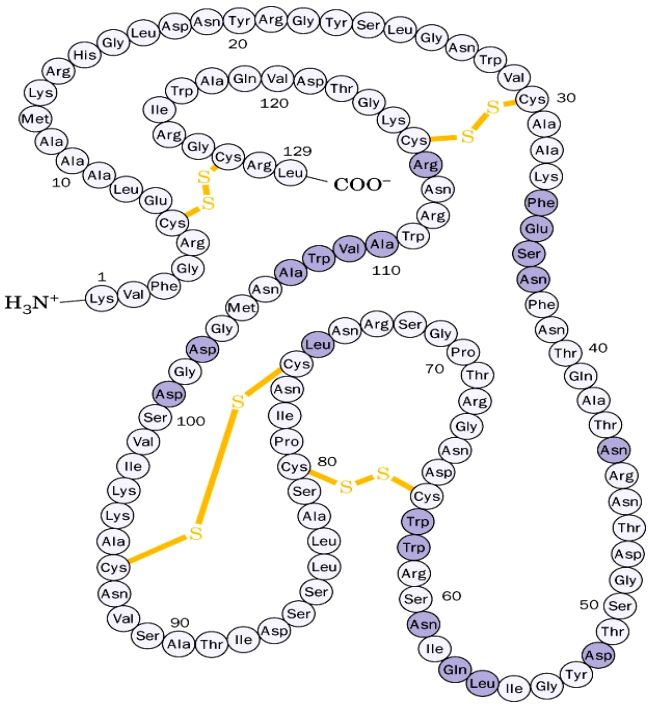

Figure 4-1: Primary structure of Hen Egg White Lysozyme

References

1. Davies, J.M. **(2005)** *Biochim. Biophys. Acta.* 1703, 93-109.

2. Barry Halliwell. (**1987**) *Proceedings of the Nutrition Society,* 46, 13-26.

3. Stadtman, E. R., Levine, R. L. **(2003)** *Amino Acids.* 25, 207-218.

4. Stohs, J. S. **(1995)** J. Basic. *Clin. Physiol. Pharmacol*. 6, 205-228

5. Halliwell, B., Gutteridge, J. M. C. **(1985)** *Molec. Aspects Med.* 8, 89-193.

6. Hovorka, S. W., Williams, T.D., Schoneich, C. **(2002)** *Anal. Biochem.* 300, 206-211.

7. http://journals.ohiolink.edu/ejc/pdf.cgi/Naderi_Jafar.pdf?issn=00476374&issue= v127i0001&article=25_ciosifrtabos.

8. http://journals.ohiolink.edu/ejc/pdf.cgi/Moylan_Jennifer_S.pdf?issn=0148639x&issue= v35i0004&article=411_oscdamw.

9. Halliwell, B. **(1987)** *FASEB.* 1, 358-364.

10. Stadman, R. E., Berlett., S.B. **(1997)** *Chem. Res. Toxicol.* 10, 485-494.

11. Bordo, D., Argos, P., **(1991)** *J. Mol. Biol.* 217, 721-729.

12. Liu, T.S., Saito, A., Azakami, H., Kato. A., **(2003)** *Pro. Exp and purification.* 27, 304-312.

13. Spencer, J.A., Jeenes, J.D., Mackenzie, A.D., Haynie, T.D., Archer, B.D., **(1998)** *Eur. J. Biochem.* 258, 107-112.

14. Giulivi, C., Traaseth, J.N., Davies, K. J. A. **(2003)** *Amino acids.* 25, 227-232.

15. Clare, J.J., Rayment, F. B., Ballentine, S. P., Sreekrishna, K., Romanos, M.A., **(1991)** *Biotechnology.* 9, 455-460.

16. Yi sun., **(1990)** *Free Radical. Biol. Med.* 8, 583-599.

17. B. Fischer., B. Perry., G. Phillips., I. Sumner., P. Goodenough., **(1993)** *Appl Microbiol Biotechnol.* 39 (4-5), 537-540.

18. Li, S., Schoneich, C., Borchardt, T. R. **(1995)** *Biotechnol. Bioeng.* 48, 490-500.

19. Lim, Jihyeon., Vachet, W.R. **(2003)** *Anal. Chem.* 75 (5), 1164-1172.

20. Agil, A., Fuller, J.C., Jialal, I. **(1995)** *Clin. Chem.* 41 (2), 220-225.

21. Mine, S., Ueda. T., Hashimoto, Y., Tanaka, Y., Imoto, T., **(1999)** *FEBS Letters.* 448, 33-37.

22. Ookawara, T., Kawamura, N., Kitagawa, Y., Taniguchi, N. **(1992)** *J. Biol. Chem.* 267 (26), 18505-18510.

23. Easy select ^{TM} Pichia expression kit manual.

24. Brierly, R. A., Bussineau, C., Kosson, R., Melton, A. Siegel, R.S., **(1990)** *Ann NY Acad Sci.* 589, 350-362.

25. Koshiba, T., Hayashi, T., Miwako, I., Kumagai, I., Ikura, T., **(1999)** *Prot. Eng.* 12 (5), 429-435.

26. Uchida, K. **(2003)** *Amino Acids.* 25, 249-257.

27. http://journals.ohiolink.edu/ejc/pdf.cgi/Brouwer_M.pdf?issn=01411136&issue=v50i1-5&article=103_nfocaatucfot.

Appendix A: DNA sequence (390) and corresponding amino acid (129) sequence of hen egg white lysozyme

1-10	AAA	GTC	TTT	GGA	CGA	TGT	GAG	CTA	GCA	GCG
	Lys	Val	Phe	Gly	Arg	Cys	Glu	Leu	Ala	Ala
11-20	GCT	ATG	AAG	CGT	CAC	GGA	CTT	GAT	AAC	TAT
	Ala	Met	Lys	Arg	His	Gly	Leu	Asp	Asn	Tyr
21-30	CGG	GGA	TAC	AGC	CTG	GGA	AAC	TGG	GTG	TGT
	Arg	Gly	Tyr	Ser	Leu	Gly	Asn	Trp	Val	Cys
31-40	GCT	GCA	AAA	TTC	GAG	AGT	AAC	TTC	AAC	ACC
	Ala	Ala	Lys	Phe	Glu	Ser	Asn	Phe	Asn	Thr
41-50	CAG	GCT	ACA	AAC	CGT	AAC	ACC	GAT	GGG	AGT
	Gln	Ala	Thr	Asn	Arg	Asn	Thr	Asp	Gly	Ser
51-60	ACC	GAC	TAC	GGA	ATC	CTA	CAG	ATC	AAC	AGC
	Thr	Asp	Tyr	Gly	Ile	Leu	Gln	Ile	Asn	Ser
61-70	CGC	TGG	TGG	TGC	AAC	GAT	GGC	AGG	ACT	CCA
	Arg	Trp	Trp	Cys	Asn	Asp	Gly	Arg	Thr	Pro
71-80	GGC	TCC	AGG	AAC	CTG	TGC	AAC	ATC	CCG	TGC
	Gly	Ser	Arg	Asn	Leu	Cys	Asn	Ile	Pro	Cys
81-90	TCA	GCC	CTG	CTG	AGC	TCA	GAC	ATA	ACA	GCG
	Ser	Ala	Leu	Leu	Ser	Ser	Asp	Ile	Thr	Ala
91-100	AGC	GTG	AAC	TGT	GCG	AAG	AAG	ATC	GTC	AGC
	Ser	Val	Asn	Cys	Ala	Lys	Lys	Ile	Val	Ser
101-110	GAT	GGA	AAC	GGC	ATG	AAC	GCG	TGG	GTC	GCC
	Trp	Arg	Asn	Arg	Cys	Lys	Gly	Thr	Asp	Val
111-120	TGG	CGC	AAC	CGC	TGC	AAG	GGT	ACC	GAC	GTC
	Trp	Arg	Asn	Arg	Cys	Lys	Gly	Thr	Asp	Val
121-129	CAG	GCG	TGG	ATC	AGA	GGC	TGC	CGG	CTC	TAG
	Gln	Ala	Trp	Ile	Arg	Gly	Cys	Arg	Leu	Stop